2022 American Control Conference (ACC)
Atlanta, USA, June 8-10, 2022

Robust Learning-Based Trajectory Planning for Emerging Mobility Systems

Behdad Chalaki, *IEEE Student Member*, Andreas A. Malikopoulos, *IEEE Senior Member*

***Abstract*— In this paper, we extend a framework that we developed earlier for coordination of connected and automated vehicles (CAVs) at a signal-free intersection to incorporate uncertainty. Using the possibly noisy observations of actual time trajectories and leveraging Gaussian process regression, we learn the bounded confidence intervals for deviations from the nominal trajectories of CAVs online. Incorporating these confidence intervals, we reformulate the trajectory planning as a robust coordination problem, the solution of which guarantees that constraints in the system are satisfied in the presence of bounded deviations from the nominal trajectories. We demonstrate the effectiveness of our extended framework through a numerical simulation.**

I. Introduction

THROUGH the advancements of communication technologies and computational capabilities, we are transitioning to an *emerging mobility system*, in which connected and automated vehicles (CAVs) can make better decisions leading to reductions of energy consumption, travel delays, and improvements to passengers safety [1].

After the seminal work of Athans [2] on safely coordinating vehicles at merging roadways, several research efforts have explored the benefits of coordinating CAVs in traffic scenarios using a bi-level framework which consists of (1) an *upper-level* optimization that yields, for each CAV, the optimal time to exit a predetermined control zone of the intersection [3]–[11]; and (2) a *low-level* optimization that yields for the CAV its optimal control input (acceleration/deceleration) to achieve the optimal time derived in the upper-level subject to the state, control, and safety constraints. Given the solution of the upper-level optimization problem, the low-level optimization for each CAV addresses a constrained optimal control problem using model predictive control (MPC) [9], [12]–[15], or standard optimal control techniques resulting in closed-form analytical solutions [3], [16]–[18]. However, the latter approach leads to a system of non-linear equations that might be challenging, in some instances, to solve in real time. To address this problem, a different approach was recently proposed in [17] consisting of a single optimization level aimed at both minimizing energy consumption and improving the traffic throughput. In this approach, each CAV computes the optimal exit time of the control zone corresponding to an unconstrained energy optimal trajectory which satisfies all the state, control, and safety constraints.

Although there have been several studies addressing the problem of coordination of CAVs, only a limited number of papers considers uncertainty. Xiao et al. [19] employed a control barrier function (CBF) to track the optimal control trajectory in the presence of noise process in the model. Zhou et al. [20] proposed a centralized receding horizon stochastic optimal control strategy for cooperative adaptive cruise control of platoons of vehicles to incorporate noise in the system dynamics and measurements.

In this paper, we build upon the framework introduced in [17] and enhance it by reformulating the coordination of CAVs as a robust coordination problem. We employ Gaussian process (GP) regression to learn the deviation of CAVs from their nominal time trajectory and obtain confidence intervals on the unknown errors of nominal trajectories based on the noisy observations of CAVs. The obtained confidence intervals can then be used to solve the robust coordination problem using a worst-case scenario approach. A GP is defined as a collection of random variables, any finite number of which have a joint Gaussian distribution, and can be used to describe a distribution over an infinite-dimensional space of functions [21]. GP models have been used in various control applications, including ship trajectory prediction [22], modeling and control of buildings [23], and safe-learning for ground and aerial vehicles [24]–[26].

We believe that this paper advances the state of the art in the following ways. First, rather than not considering uncertainty for the vehicle's trajectory planning [3], [8], [9], [12]–[15], [17], [18] or assuming a known bound [16], we employ GP regression to model uncertainty and incorporate it in our coordination framework. Second, by considering uncertainty in the vehicle's trajectory planning, we ensure safety in the presence of uncertainty without sacrificing optimality, in contrast to the methods with reactive mechanisms such as CBF [19] which can potentially result in an optimality gap.

The rest of the paper is structured as follows. In Section II, we introduce the modeling framework, and in Section III, we present the solution approach. We provide simulation results in Section IV, and concluding remarks in Section V.

II. Problem Formulation

We consider a signal-free intersection, which includes a *coordinator* that stores information about the intersection's geometry and CAVs' trajectories (Fig. 1). The coordinator does not make any decision, and it only acts as a *database* for the CAVs. The intersection includes a *control zone* inside of

This research was supported in part by ARPAE's NEXTCAR program under the award number DE- AR0000796 and by the Delaware Energy Institute (DEI). This support is gratefully acknowledged.

The authors are with the Department of Mechanical Engineering, University of Delaware, Newark, DE 19716 USA (emails: {bchalaki;andreas}@udel.edu).

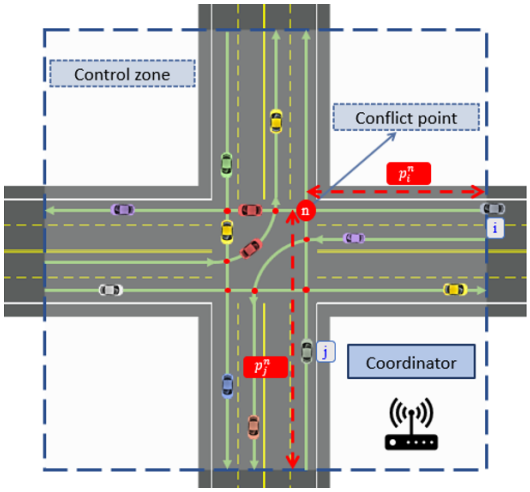

Fig. 1: A signal free intersection with conflict points.

which the CAVs can communicate with the coordinator. We call the points inside the control zone where paths of CAVs intersect and a lateral collision may occur *conflict points*. Let $\mathcal{L} \subset \mathbb{N}$ indexes the set of conflict points, $N(t) \in \mathbb{N}$ be the total number of CAVs inside the control zone at time $t \in \mathbb{R}_{\geq 0}$, and $\mathcal{N}(t) = \{1, \ldots, N(t)\}$ be the queue that designates the order in which each CAV entered the control zone. We model the dynamics of each CAV $i \in \mathcal{N}(t)$ as

$$\begin{aligned} \dot{p}_i(t) &= v_i(t), \\ \dot{v}_i(t) &= u_i(t), \end{aligned} \tag{1}$$

where $p_i(t) \in \mathcal{P}_i$, $v_i(t) \in \mathcal{V}_i$, and $u_i(t) \in \mathcal{U}_i$ denote position, speed, and control input at t, respectively. The sets $\mathcal{P}_i$, $\mathcal{V}_i$, and $\mathcal{U}_i$, $i \in \mathcal{N}(t)$, are compact subsets of $\mathbb{R}$. Let $t_i^0 \in \mathbb{R}_{\geq 0}$ and $t_i^f > t_i^0 \in \mathbb{R}_{\geq 0}$ be the time that CAV $i \in \mathcal{N}(t)$ enters and exits the control zone, respectively. For each CAV $i \in \mathcal{N}(t)$ the control input and speed are bounded by

$$u_{i,\min} \leq u_i(t) \leq u_{i,\max}, \tag{2}$$

$$0 < v_{\min} \leq v_i(t) \leq v_{\max}, \tag{3}$$

where $u_{i,\min}, u_{i,\max}$ are the minimum and maximum control inputs and $v_{\min}, v_{\max}$ are the minimum and maximum speed limit, respectively.

To guarantee rear-end safety between CAV $i \in \mathcal{N}(t)$ and the preceding CAV $k \in \mathcal{N}(t) \setminus \{i\}$, we have

$$p_k(t) - p_i(t) \geq \delta_i(t) = \gamma + \varphi \cdot v_i(t), \tag{4}$$

where $\delta_i(t)$ is the safe speed-dependent distance, while γ and $\varphi \in \mathbb{R}_{>0}$ are the standstill distance and reaction time, respectively.

Definition 1. *For CAV $i \in \mathcal{N}(t)$, the inverse function, p_i^{-1} is the time trajectory and denoted by $t_i \colon \mathcal{P}_i \to [t_i^0, t_i^f]$. The time trajectory yields the time that CAV i is at position $p_i \in \mathcal{P}_i$ inside the control zone.*

Since $0 < v_{\min} \leq v_i(t)$, the position $p_i(t)$ is a strictly increasing function. Moreover, for every element in $\mathcal{P}_i$, there is at least one element in $[t_i^0, t_i^f]$, which implies that the position $p_i(t)$ is a surjective function [17], and hence the inverse $t_i(\cdot) = p_i^{-1}(\cdot)$ exists.

CAV i may have a lateral collision with CAV $j \in \mathcal{N}(t) \setminus \{i\}$ at conflict point $n \in \mathcal{L}$ (Fig. 1). We denote by p_i^n and p_j^n the distance of the conflict point n from i's and j's paths' entries, respectively (Fig. 1). To guarantee lateral collision avoidance, we impose the following time headway constraint

$$\left| t_i(p_i^n) - t_j(p_j^n) \right| \geq t_h, \tag{5}$$

where $t_h \in \mathbb{R}_{>0}$ is the minimum time headway between any two CAVs crossing conflict point n.

A. Deterministic Coordination Problem

We first review the single-level optimization framework for coordination of CAV developed in [17]. Upon entrance, each CAV $i \in \mathcal{N}(t)$ communicates with the coordinator to access the time trajectories of CAVs which are already in the control zone. After obtaining this information, CAV i solves a time minimization problem to determine the time that it must exit the control zone, t_i^f. The time t_i^f corresponds to the unconstrained energy optimal trajectory guaranteeing that state, control, and safety constraints are satisfied. This trajectory is communicated back to the coordinator, so that the subsequent CAVs receive this information and plan their trajectories accordingly.

The unconstrained energy optimal solution of CAV i which has the following form [17]

$$\begin{aligned} p_i(t) &= \phi_{i,3} \cdot t^3 + \phi_{i,2} \cdot t^2 + \phi_{i,1} \cdot t + \phi_{i,0}, \\ v_i(t) &= 3\phi_{i,3} \cdot t^2 + 2\phi_{i,2} \cdot t + \phi_{i,1}, \\ u_i(t) &= 6\phi_{i,3} \cdot t + 2\phi_{i,2}, \end{aligned} \tag{6}$$

where $\phi_{i,3} \neq 0$ and $\phi_{i,2}, \phi_{i,1}, \phi_{i,0} \in \mathbb{R}$ are the constants of integration. CAV i must also satisfy the boundary conditions

$$p_i(t_i^0) = 0, \;\; v_i(t_i^0) = v_i^0, \;\; p_i(t_i^f) = p_i^f, \;\; u_i(t_i^f) = 0, \tag{7}$$

where $u_i(t_i^f) = 0$ because the speed at the exit of the control zone is not specified [27].

Using the Cardano's method [28], $t_i(p_i)$ is given by

$$\begin{aligned} t_i(p_i) = \; & \sqrt[3]{-\frac{1}{2}\left(\omega_{i,1} + \omega_{i,2}\, p_i\right) + \sqrt{\frac{1}{4}\left(\omega_{i,1} + \omega_{i,2}\, p_i\right)^2 + \frac{1}{27}\omega_{i,0}^3}} + \\ & \sqrt[3]{-\frac{1}{2}\left(\omega_{i,1} + \omega_{i,2}\, p_i\right) - \sqrt{\frac{1}{4}\left(\omega_{i,1} + \omega_{i,2}\, p_i\right)^2 + \frac{1}{27}\omega_{i,0}^3}} \\ & + \omega_{i,3}, \qquad p_i \in \mathcal{P}_i, \end{aligned} \tag{8}$$

where $\omega_{i,3}, \omega_{i,2}, \omega_{i,1}$, and $\omega_{i,0} \in \mathbb{R}$ such that $\frac{1}{4}(\omega_{i,1} + \omega_{i,2}\, p_i)^2 + \frac{1}{27}\omega_{i,0}^3 > 0$, and they are all defined in terms of $\phi_{i,3}, \phi_{i,2}, \phi_{i,1}, \phi_{i,0}$ [17]. We formally define the single-level optimization framework as follows.

Problem 1. *Each CAV $i \in \mathcal{N}(t)$ solves the following optimization problem at t_i^0, upon entering the control zone*

$$\min_{t_i^f \in \mathcal{T}_i(t_i^0)} \; t_i^f \tag{9}$$

subject to: (4) – (8),

where the compact set $\mathcal{T}_i(t_i^0)$ is the set of feasible solution of CAV $i \in \mathcal{N}(t)$ for the exit time computed at t_i^0 using the speed and control input constraints (2)-(3), and boundary conditions (7). Refer to [29] for further details.

B. Uncertainty in the Coordination Problem

In an earlier work [29], we showed that there is a discrepancy between the actual and planned trajectories due to the presence of uncertainty originated from error in low-level tracking, noisy measurements, etc. In this paper, to accommodate this uncertainty, we reformulate Problem 1 as a robust coordination problem, the solution of which guarantees that constraints in the system are satisfied in the presence of bounded deviations from the nominal trajectories.

Assumption 1. *The deviation from the deterministic nominal time trajectory of a real-physical CAV $i \in \mathcal{N}(t)$ is given by an unknown function $e_i : \mathcal{P}_i \to \mathcal{E}_i$, where $\mathcal{E}_i$ is an unknown bounded subset of $\mathbb{R}$.*

We consider that $e_i(p_i)$ can be approximated by a GP defined on a probability space $(\mathcal{P}_i, \mathscr{P}_i, \mathbb{P})$, where $\mathscr{P}_i$ is the associated σ-algebra and $\mathbb{P}$ is a probability measure on $(\mathcal{P}_i, \mathscr{P}_i)$. This is a reasonable approach, since GP regression has been used successfully to approximate functions in many applications [21].

Definition 2. *The actual time trajectory for CAV $i \in \mathcal{N}(t)$ is a random process defined on $(\mathcal{P}_i, \mathscr{P}_i, \mathbb{P})$, denoted by $\hat{t}_i : \mathcal{P}_i \to \mathbb{R}$, and given by*

$$\hat{t}_i(p_i) = t_i(p_i) + e_i(p_i), \tag{10}$$

where $t_i(p_i)$ is the nominal trajectory which is the solution of Problem 1.

From Definition 1, the time trajectory is the inverse function of the position trajectory. Having a deviation in the time trajectory also makes the deviation in the position trajectory inevitable.

Definition 3. *The actual position trajectory of CAV $i \in \mathcal{N}(t)$ is a random process denoted by $\hat{p}_i$ defined on a probability space $(\Omega_i, \mathscr{F}_i, \mathbb{P})$, $\Omega_i \in \mathbb{R}$, and given by*

$$\hat{p}_i(t) = p_i(t) + f_i(t), \tag{11}$$

where $f_i(t)$ is the unknown deviation from the nominal position trajectory, and it is defined on $(\Omega_i, \mathscr{F}_i, \mathbb{P})$.

Lemma 1. *The deviation in the position trajectory of CAV $i \in \mathcal{N}(t)$, $f_i(t)$, can be derived from the deviation $e_i(t)$ of its time trajectory.*

Proof. Let $p_i \in \mathcal{P}_i$ be an arbitrary known position, with $p_i = p_i(t)$. By evaluating (10) at p_i, we obtain the actual time $\hat{t}_i(p_i)$ that CAV $i \in \mathcal{N}(t)$ is at position p_i. Evaluating (11) at the actual time, we obtain

$$\hat{p}_i(\hat{t}_i(p_i)) = p_i(\hat{t}_i(p_i)) + f_i(\hat{t}_i(p_i)). \tag{12}$$

By definition of inverse function $(p_i \circ p_i^{-1})(x) = x$, and thus LHS in (12) equals to p_i. Substituting (10) in the first term of RHS, we have

$$\begin{aligned} p_i = \phi_{i,3} \cdot (t_i(p_i) + e_i(p_i))^3 + \phi_{i,2} \cdot (t_i(p_i) + e_i(p_i))^2 \\ + \phi_{i,1} \cdot (t_i(p_i) + e_i(p_i)) + \phi_{i,0} + f_i(\hat{t}_i(p_i)). \end{aligned} \tag{13}$$

Next, by expanding (13), we get

$$\begin{aligned} f_i(\hat{t}_i(p_i)) = -[\phi_{i,3} \cdot e_i(p_i)^3 + 3\phi_{i,3} \cdot e_i(p_i)^2 \cdot t_i(p_i) \\ + \phi_{i,2} \cdot e_i(p_i)^2 + 3\phi_{i,3} \cdot e_i(p_i) \cdot t_i(p_i)^2 \\ + 2\phi_{i,2} \cdot e_i(p_i) \cdot t_i(p_i) + \phi_{i,1} \cdot e_i(p_i)]. \end{aligned} \tag{14}$$

Since $p_i \in \mathcal{P}_i$ is an arbitrary known position, the above equation holds for any p_i, and the proof is complete. □

Corollary 1. *The actual speed trajectory of CAV $i \in \mathcal{N}(t)$, $\hat{v}_i(t)$ is a random process defined on probability space $(\Omega_i, \mathscr{F}_i, \mathbb{P})$, and it is found from*

$$\hat{v}_i(t) = v_i(t) + g_i(t), \tag{15}$$

where $g_i(t)$ is unknown deviation from nominal speed trajectory, and is defined on $(\Omega_i, \mathscr{F}_i, \mathbb{P})$.

Proof. By taking time derivative of (11), the result follows immediately. □

C. Robust Coordination Problem

For each CAV $i \in \mathcal{N}(t)$, we formulate a robust coordination problem in the presence of uncertainty. We seek to derive the new minimum time t_i^f for CAV i to exit the control zone. This exit time corresponds to a new unconstrained energy-optimal trajectory that satisfies all the state, control, and safety constraints for all realizations of uncertainty. In what follows, let $E_i(\cdot) \subset \mathcal{E}_i$, $F_i(\cdot) \subset \mathcal{P}_i$, $G_i(\cdot) \subset \mathcal{V}_i$ denote the bounded confidence intervals of CAV i for random process $e_i(\cdot)$, $f_i(\cdot)$, and $g_i(\cdot)$, respectively.

We enhance (5) as follows

$$\begin{aligned} &\left|\hat{t}_i(p_i^n) - \hat{t}_j(p_j^n)\right| \geq t_h, \\ &\forall e_i(p_i^n) \in E_i(p_i^n), \forall e_j(p_j^n) \in E_j(p_j^n), \end{aligned} \tag{16}$$

to include the CAVs' deviations from their nominal time trajectories.

Similarly, we enhance rear-end safety constraint (4) defined on the nominal trajectories by incorporating the deviations from nominal position trajectories (11) as follows

$$\begin{aligned} &\hat{p}_k(t) - \hat{p}_i(t) \geq \hat{\delta}_i(t) = \gamma + \varphi \cdot \hat{v}_i(t), \\ &\forall f_i(t) \in F_i(t),\ \forall f_k(t) \in F_k(t),\ \forall g_i(t) \in G_i(t), \end{aligned} \tag{17}$$

where the distance between CAV $i \in \mathcal{N}(t)$ and the preceding CAV $k \in \mathcal{N}(t) \setminus \{i\}$ has to be greater than a safe distance $\hat{\delta}_i(t)$ for every realizations of deviations from the nominal trajectories of CAV i and CAV k (Fig. 1). Finally, to account for the deviation of the speed of CAV i, we enhance the constraint

$$v_{\min} \leq \hat{v}_i(t) \leq v_{\max}, \quad \forall g_i(t) \in G_i(t). \tag{18}$$

Problem 2. *For each CAV $i \in \mathcal{N}(t)$, we consider the following robust coordination problem*

$$\min_{t_i^f \in \mathcal{T}_i(t_i^0)} t_i^f \tag{19}$$
$$\text{subject to: } (6), (8), (10), (11), (15) - (18),$$
$$\text{and given boundary conditions.}$$

In what follows, to simplify notation, for CAV $i \in \mathcal{N}(t)$, we denote the original nominal trajectories (resulting from the solution of Problem 1) with bar, e.g., $\bar{t}_i(p_i), \bar{p}_i(t), \bar{v}_i(t)$, and $\bar{u}_i(t)$, and reserve $t_i(p_i), p_i(t), v_i(t)$, and $u_i(t)$ for the new nominal trajectories (resulting from the solution of Problem 2).

III. Solution approach

In our framework, upon entering the control zone, CAV $i \in \mathcal{N}(t)$ does not have any information about its uncertainty, and thus we have $E_i(\cdot) = F_i(\cdot) = G_i(\cdot) = \emptyset$. First, CAV i communicates with the coordinator and obtain trajectories and information about the uncertainty of CAVs which are already in the control zone. Using this information, CAV i computes its nominal trajectories by solving Problem 2. As CAV i travels following these nominal trajectories, it makes measurements (possibly noisy) of the actual time that it reaches to different positions $p_i \in \mathcal{P}_i$, denoted by $\tilde{t}_i(p_i) \in \mathbb{R}_{\geq 0}$, and given by $\tilde{t}_i(p_i) = \hat{t}_i(p_i) + \xi_i$, where $\xi_i \sim \mathcal{N}(0, \sigma_n^2)$ is a Gaussian noise with unknown variance σ_n^2. Next, we define the error in the time trajectory based on these measurements.

Definition 4. *The difference between the noisy measurements of the time trajectory $\tilde{t}_i(p_i)$ and the nominal time trajectory $t_i(p_i)$ is denoted by $\tilde{e}_i(p_i) = \tilde{t}_i(p_i) - t_i(p_i)$, which is a random process on a probability space $(\mathcal{P}_i, \mathscr{P}_i, \mathbb{P})$.*

The set of observation samples of CAV $i \in \mathcal{N}(t)$, is denoted by $\mathcal{O}_i = (\mathbf{p}_i, \tilde{\mathbf{e}}_i) = \left\{ \left(p_i^{(j)}, \tilde{e}_i(p_i^{(j)}) \right) \mid j = 1, \ldots, n \right\}$, where $\mathbf{p}_i$, $\tilde{\mathbf{e}}_i$ represent the n dimensional vector of positions and corresponding observed errors in time trajectory; respectively, and the jth sample is denoted by $\left(p_i^{(j)}, \tilde{e}_i(p_i^{(j)}) \right)$. We consider that CAV i makes the noisy observations $\mathcal{O}_i$ before reaching a perfectly known landmark in the control zone called *uncertainty characterization point* denoted by $p^z \in \mathcal{P}_i$. Let t_i^z be the actual time that CAV i reaches this point. After CAV i reaches p^z, it characterizes its uncertainty in the time, position, and speed trajectories based on the observed information, $\mathcal{O}_i$. Then, CAV i communicates with the coordinator to access the trajectories of other CAVs $j < i \in \mathcal{N}(t)$ which entered the control zone earlier than CAV i. CAV i also obtains information about their deviation from their trajectories, if they have already characterized their uncertainty. After obtaining this information, CAV i solves the robust coordination problem (Problem 2), with the revised initial conditions $p_i(t_i^z) = p^z$ and $v_i(t_i^z) = \bar{v}_i(t_i^z) + g(t_i^z)$ (recall that $\bar{v}_i(t_i^z)$ is the speed of CAV i at t_i^z computed from the original nominal trajectory). CAV i communicates back these new nominal trajectories along with its characterization of uncertainty to the coordinator. Then, the coordinator broadcasts a *replanning event* for all CAVs $j > i \in \mathcal{N}(t)$ which entered the control zone after CAV i to re-plan their trajectory with this new information. These CAVs then sequentially resolve their optimization problem, and plan their trajectory accordingly.

Given the observation samples, $\mathcal{O}_i$, we use GP regression to model $e_i(p_i) \sim \mathcal{GP}(m(p_i), k(p_i, p_i'))$, where $m(p_i)$ and $k(p_i, p_i')$ represents the prior mean and covariance, respectively. We assume no prior knowledge on the error is available, and thus, we set the prior mean to zero, $m(p_i) = 0$. For the covariance function, we adopt the *Matérn* $3/2$ model that is one time differentiable in the mean-square sense, and it is given by $k(p_i, p_i') = \frac{\sigma_s^2}{\Gamma(\frac{3}{2})} \left(\sqrt{3} \frac{p_i - p_i'}{\ell_s} \right)^{\frac{3}{2}} K_{\frac{3}{2}} \left(\sqrt{3} \frac{p_i - p_i'}{\ell_s} \right)$, where $K_{\frac{3}{2}}$ and Γ are modified Bessel and Gamma functions, respectively. Let σ_s^2 and ℓ_s be the process variance, the covariance function's parameter, respectively [21]. The hyperparameters are represented by $\theta = [\sigma_s^2 \ \sigma_n^2 \ \ell_s]^\top$, where σ_n^2 is the unknown variance of observation noise. The hyperparameters can be learned by maximizing the log marginal likelihood of the observation samples, i.e., $\theta^* = \arg\max_\theta \log \mathbb{P}(\tilde{\mathbf{e}}_i | \mathbf{p}_i, \theta)$. Given the observation samples, $\mathcal{O}_i$, the marginalized GP posterior at any arbitrary point p_i^* is a univariate normal distribution, denoted by $e_i(p_i^*) \sim \mathcal{N}(\mu_e(p_i^*), \sigma_e^2(p_i^*))$ defined with the mean $\mu_e(p_i^*) = m(p_i^*) + k^*(K + \sigma_n^2 I)^{-1} \tilde{\mathbf{e}}_i$ and variance $\sigma_e^2(p_i^*) = k(p_i^*, p_i^*) - k^{*\top}(K + \sigma_n^2 I)^{-1} k^*$, where $K = K(\mathbf{p}_i, \mathbf{p}_i)$ denotes the $n \times n$ matrix of the covariances evaluated at all pairs of training point $\mathbf{p}_i$, and $k^* = K(\mathbf{p}_i, p_i^*)$ is the $n \times 1$ matrix of the covariances evaluated at n training points and one arbitrary point, p_i^*.

Theorem 1. *Deviation from the nominal speed trajectory of CAV $i \in \mathcal{N}(t)$, $g_i(t)$, follows a Chi-square distribution with one degree of freedom, and its posterior mean and variance at actual time $\hat{t}_i(p_i)$, where CAV arrives at position p_i can be derived from $\mu_g(\hat{t}_i(p_i)) = a_1' \, \mu_e + a_2' \left(\mu_e^2 + \sigma_e^2 \right)$ and*

$$\sigma_g^2(\hat{t}_i(p_i)) = \sigma_e^2 \left({a_1'}^2 + 4\mu_e(a_1' \, a_2' + {a_2'}^2 \, \mu_e) + 2 \, {a_2'}^2 \, \sigma_e^2 \right), \tag{20}$$

where $a_1' = -2\phi_{i,2} - 6\phi_{i,3} \cdot t_i(p_i)$ and $a_2' = -3\phi_{i,3}$, and $\mu_e = \mu_e(p_i)$, $\sigma_e = \sigma_e(p_i)$.

Proof. Let $p_i \in \mathcal{P}_i$ be an arbitrary known position, with $p_i = p_i(t)$ and $\hat{t}_i(p_i)$ be the actual time, where CAV arrives at position p_i. Following the same steps as Lemma 1, the deviation is given by $g_i(\hat{t}_i(p_i)) = -[(2\phi_{i,2} + 6\phi_{i,3} \cdot t_i(p_i)) \cdot e_i(p_i) + 3\phi_{i,3} \cdot e_i(p_i)^2]$, where $e_i(p_i)$ is a univariate normal variable, and thus $g_i(\hat{t}_i(p_i))$ follows a Chi-square distribution with one degree of freedom [30]. Since $e_i(p_i)$ is a normal random variable, its moment-generating function is given by $M_e(\tau) = \exp(\tau\mu_e + \frac{1}{2}\sigma_e^2\tau^2)$. The nth moment of random variable $e_i(p_i)$, denoted by $\mathbb{E}[e_i(p_i)^n]$, can be derived from $\frac{d^n}{d\tau^n} M_e(\tau) \mid_{\tau=0}$. From linearity of expectation, we have $\mu_g(\hat{t}_i(p_i)) = \mathbb{E}[g_i(\hat{t}_i(p_i))] = a_1' \, \mathbb{E}[e_i(p_i)] + a_2' \, \mathbb{E}[e_i(p_i)^2]$,

where the first and second moments of $e_i(p_i)$, are given by μ_e and $\mu_e^2 + \sigma_e^2$, respectively. To find the variance, we use $\sigma_g^2(\hat{t}_i(p_i)) = \mathbb{E}[g_i(\hat{t}_i(p_i))^2] - \mathbb{E}[g_i(\hat{t}_i(p_i))]^2$, where we can employ the same procedure and derive (20). □

Corollary 2. *The deviation $f_i(t)$ from the nominal position trajectory of CAV $i \in \mathcal{N}(t)$ follows a cubic normal distribution.*

Proof. Let $p_i \in \mathcal{P}_i$ be an arbitrary known position, with $p_i = p_i(t)$ and $\hat{t}_i(p_i)$ be the actual time, where CAV arrives at position p_i. From (14), we have $f_i(\hat{t}_i(p_i)) = a_3 \cdot e_i(p_i)^3 + a_2 \cdot e(p_i)^2 + a_1 \cdot e_i(p_i)$, where $e_i(p_i)$ is a normal variable,-

$$a_1 = -3\phi_{i,3} \cdot t_i(p_i)^2 - 2\phi_{i,2} \cdot t_i(p_i) - \phi_{i,1}, \tag{21}$$

$$a_2 = -3\phi_{i,3} \cdot t_i(p_i) - \phi_{i,2}, \tag{22}$$

and $a_3 = -\phi_{i,3}$. Since a_1, a_2, and a_3 are not random variables, the proof is complete. □

Proposition 1. *For CAV $i \in \mathcal{N}(t)$, posterior mean and variance of $f_i(t)$ at actual time $\hat{t}_i(p_i)$, where vehicle arrives at position p_i can be derived from*

$$\mu_f(\hat{t}_i(p_i)) = a_1\mu_e + a_3(\mu_e^3 + 3\mu_e\sigma_e^2) + a_2(\mu_e^2 + \sigma_e^2) \tag{23}$$

$$\begin{aligned}\sigma_f^2(\hat{t}_i(p_i)) = \sigma_e^2[{a_1}^2 + 4a_1a_2\mu_e + 6a_1a_3\mu_e^2 + 6a_1a_3\sigma_e^2 + \\ 4{a_2}^2\mu_e^2 + 2{a_2}^2\sigma_e^2 + 12a_2a_3\mu_e^3 + 24a_2a_3\mu_e\sigma_e^2 \\ +9{a_3}^2\mu_e^4 + 36{a_3}^2\mu_e^2\sigma_e^2 + 15{a_3}^2\sigma_e^4],\end{aligned} \tag{24}$$

where $\mu_e = \mu_e(p_i)$, $\sigma_e = \sigma_e(p_i)$.

Proof. The proof is similar to Theorem 1, hence it is omitted. □

Next, we construct a bounded confidence interval for random process $e_i(p_i)$, denoted by $E_i(p_i) \subset \mathcal{E}_i$, within which $e_i(p_i)$ lies with probability P_e as $E_i(p_i) = [\mu_e(p_i) - z\sigma_e(p_i),\ \mu_e(p_i) + z\sigma_e(p_i)]$, $z = \sqrt{2}\,\mathrm{erf}^{-1}(P_e)$ where $\mu_e(p_i)$ and $\sigma_e(p_i)$ are posterior mean and standard deviation of $e_i(p_i)$ at position $p_i \in \mathcal{P}_i$, respectively, and $\mathrm{erf}^{-1}(\cdot)$ is the inverse error function. Using Chebyshev's inequality, we construct a bounded confidence interval for the random process $f_i(t)$, denoted by $F_i(t) \subset \mathcal{P}_i$, within which $f_i(t)$ lies with at least probability P_f as $F_i(p_i) = [\mu_f(t) - z\sigma_f(t),\ \mu_f(t) + z\sigma_f(t)]$, where $\mathbb{P}(f_i(t) \in F_i(t)) \geq P_f = 1 - \frac{1}{z^2}$.

Deviation from speed trajectory, $g_i(t)$, follows a Chi-squared distribution which is a uni-modal distribution, i.e., its distribution permits a Lebesgue density that is non-decreasing up to a mode and non-increasing thereafter. This unimodality allows us to employ a tighter bound for the confidence interval using Vysochanskii-Petunin inequality [31]. We construct a bounded confidence interval for the random process $g_i(t)$, denoted by $G_i(t) \subset \mathcal{V}_i$, within which $g_i(t)$ lies with at least probability P_g as $G_i(p_i) = [\mu_g(t) - z\sigma_g(t),\ \mu_g(t) + z\sigma_g(t)]$ where $\mathbb{P}(g_i(t) \in G_i(t)) \geq P_g = 1 - \frac{4}{9z^2}$. The solution to Problem 2 is the optimal nominal trajectories for CAV $i \in \mathcal{N}(t)$ satisfying the safety constraints in the presence of uncertainty, which is modeled through GP based on the possibly noisy observations of the time trajectory.

IV. Simulation Results

To demonstrate the effectiveness of our proposed framework, we investigate the coordination of 24 CAVs at a signal-free intersection shown in fig.1. The CAVs enter the control zone from 6 different paths shown in fig. 1 with the total rate of 3600 veh/hour and their initial speeds uniformly distributed between 12 m/s to 14 m/s. We use the following parameters for the simulation: $t_h = 0.5$ s, $v_{\min} = 0.25$ m/s, $v_{\max} = 30$ m/s, $u_{\max} = 2$ m/s^2, $u_{\min} = -2$ m/s^2, $\gamma = 1.5$ m, $\varphi = 0.5$ s, $p^z = 50$ m, $P_e = P_f = P_g = 95\%$. We consider the actual deviation from the nominal time trajectory for CAV $i \in \mathcal{N}(t)$ is given by function $e_i(p_i) = 0.012 \log(1 + p_i)^{1.5}$ which is not known to CAV i a priori. Videos from our simulation analysis can be found at the supplemental site, https://sites.google.com/view/ud-ids-lab/RBST.

Fig. 2 illustrates time trajectories of CAVs traveling from westbound to eastbound. The CAVs nominal trajectories on this path are denoted with solid lines, while their corresponding rear-end safety constraints (17) are visualized with dotted lines in the same color. Replanning events that are due to the change of the trajectories of other CAVs in the control zone are shown with blue asterisks, and the uncertainty characterization point at which each CAV quantifies its trajectory is shown with a black square marker. The 95% confidence bounds of the time trajectories are shown with dashed lines. Moreover, the CAVs from other paths that have the potential for lateral collision with CAVs in this path are shown with vertical thicker lines. Their arrival times at the conflict points with 95% confidence bound are shown in red, and corresponding lateral safety constraints (16) are shown with vertical black lines. This figure shows that by using our robust framework, CAVs' nominal trajectories satisfy the safety constraints for every realization of the deviations from the nominal trajectories. Fig. 3 visualizes the case where CAVs stick to their initial planned nominal trajectories, ignoring uncertainty. It can be seen that for multiple cases, the trajectories of the CAVs with 95% confidence bounds cross the vertical lines representing the lateral constraints.

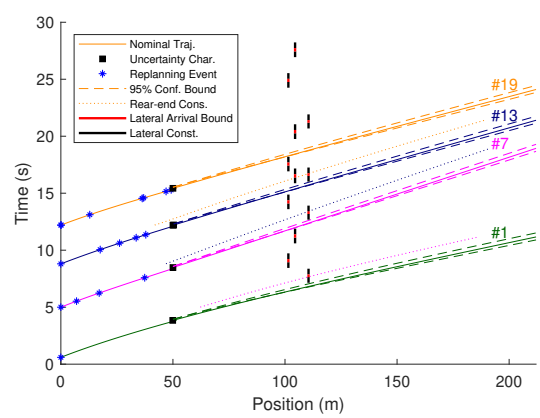

Fig. 2: Time trajectories of CAVs under robust coordination.

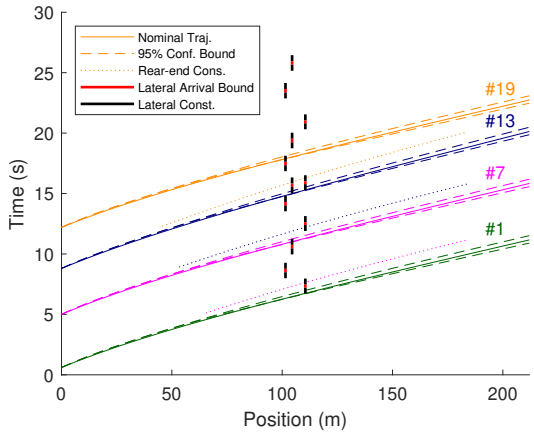

Fig. 3: Time trajectories of CAVs under deterministic coordination.

V. Concluding Remarks and Discussion

In this paper, we extended a framework we developed earlier for coordination of CAVs in [17] to include the deviations from the nominal trajectories as uncertainty and reformulated it as a robust coordination problem. We adopted the data-driven approach, GP regression, to learn the uncertainty from the possibly noisy observation of CAVs' time trajectories. After obtaining the statistical knowledge about the deviation from nominal trajectories, we constructed the confidence interval for time, position, and speed trajectories using the inverse error function, Chebyshev's inequality, and Vysochanskii-Petunin inequality, respectively. We, finally, demonstrated the effectiveness of our proposed framework through a numerical simulation. A potential directions for future research include validating the proposed framework in an experimental testbed.

References

[1] Z. Wadud, D. MacKenzie, and P. Leiby, "Help or hindrance? the travel, energy and carbon impacts of highly automated vehicles," *Transportation Research Part A: Policy and Practice*, vol. 86, pp. 1–18, 2016.

[2] M. Athans, "A unified approach to the vehicle-merging problem," *Transportation Research*, vol. 3, no. 1, pp. 123–133, 1969.

[3] A. A. Malikopoulos, C. G. Cassandras, and Y. Zhang, "A decentralized energy-optimal control framework for connected automated vehicles at signal-free intersections," *Automatica*, vol. 93, pp. 244–256, 2018.

[4] J. Rios-Torres and A. A. Malikopoulos, "Automated and Cooperative Vehicle Merging at Highway On-Ramps," *IEEE Transactions on Intelligent Transportation Systems*, vol. 18, no. 4, pp. 780–789, 2017.

[5] L. E. Beaver, B. Chalaki, A. M. Mahbub, L. Zhao, R. Zayas, and A. A. Malikopoulos, "Demonstration of a Time-Efficient Mobility System Using a Scaled Smart City," *Vehicle System Dynamics*, vol. 58, no. 5, pp. 787–804, 2020.

[6] H. Xu, Y. Zhang, L. Li, and W. Li, "Cooperative driving at unsignalized intersections using tree search," *IEEE Transactions on Intelligent Transportation Systems*, vol. 21, no. 11, pp. 4563–4571, 2019.

[7] H. Xu, Y. Zhang, C. G. Cassandras, L. Li, and S. Feng, "A bi-level cooperative driving strategy allowing lane changes," *Transportation research part C: emerging technologies*, vol. 120, p. 102773, 2020.

[8] M. A. Guney and I. A. Raptis, "Scheduling-based optimization for motion coordination of autonomous vehicles at multilane intersections," *Journal of Robotics*, vol. 2020, 2020.

[9] R. Hult, M. Zanon, S. Gros, and P. Falcone, "Optimal coordination of automated vehicles at intersections: Theory and experiments," *IEEE Transactions on Control Systems Technology*, vol. 27, no. 6, pp. 2510–2525, 2018.

[10] B. Chalaki and A. A. Malikopoulos, "Time-optimal coordination for connected and automated vehicles at adjacent intersections," *IEEE Transactions on Intelligent Transportation Systems*, pp. 1–16, 2021.

[11] S. A. Fayazi and A. Vahidi, "Mixed-integer linear programming for optimal scheduling of autonomous vehicle intersection crossing," *IEEE Transactions on Intelligent Vehicles*, vol. 3, no. 3, pp. 287–299, 2018.

[12] K.-D. Kim and P. R. Kumar, "An MPC-based approach to provable system-wide safety and liveness of autonomous ground traffic," *IEEE Transactions on Automatic Control*, vol. 59, no. 12, pp. 3341–3356, 2014.

[13] G. R. Campos, P. Falcone, H. Wymeersch, R. Hult, and J. Sjöberg, "Cooperative receding horizon conflict resolution at traffic intersections," in *53rd IEEE Conference on Decision and Control*. IEEE, 2014, pp. 2932–2937.

[14] M. Kloock, P. Scheffe, S. Marquardt, J. Maczijewski, B. Alrifaee, and S. Kowalewski, "Distributed model predictive intersection control of multiple vehicles," in *2019 IEEE Intelligent Transportation Systems Conference (ITSC)*. IEEE, 2019, pp. 1735–1740.

[15] Z. Du, B. HomChaudhuri, and P. Pisu, "Hierarchical distributed coordination strategy of connected and automated vehicles at multiple intersections," *Journal of Intelligent Transportation Systems*, vol. 22, no. 2, pp. 144–158, 2018.

[16] B. Chalaki and A. A. Malikopoulos, "Optimal control of connected and automated vehicles at multiple adjacent intersections," *IEEE Transactions on Control Systems Technology*, pp. 1–13, 2021.

[17] A. A. Malikopoulos, L. E. Beaver, and I. V. Chremos, "Optimal time trajectory and coordination for connected and automated vehicles," *Automatica*, vol. 125, no. 109469, 2021.

[18] Y. Zhang and C. G. Cassandras, "Decentralized optimal control of connected automated vehicles at signal-free intersections including comfort-constrained turns and safety guarantees," *Automatica*, vol. 109, p. 108563, 2019.

[19] W. Xiao, C. G. Cassandras, and C. A. Belta, "Bridging the gap between optimal trajectory planning and safety-critical control with applications to autonomous vehicles," *arXiv preprint arXiv:2008.07632*, 2020.

[20] Y. Zhou, S. Ahn, M. Chitturi, and D. A. Noyce, "Rolling horizon stochastic optimal control strategy for acc and cacc under uncertainty," *Transportation Research Part C: Emerging Technologies*, vol. 83, pp. 61–76, 2017.

[21] C. E. Rasmussen, "Gaussian processes in machine learning," in *Summer School on Machine Learning*. Springer, 2003, pp. 63–71.

[22] H. Rong, A. Teixeira, and C. G. Soares, "Ship trajectory uncertainty prediction based on a gaussian process model," *Ocean Engineering*, vol. 182, pp. 499–511, 2019.

[23] A. Jain, T. Nghiem, M. Morari, and R. Mangharam, "Learning and control using gaussian processes," in *2018 ACM/IEEE 9th International Conference on Cyber-Physical Systems (ICCPS)*. IEEE, 2018, pp. 140–149.

[24] C. J. Ostafew, A. P. Schoellig, and T. D. Barfoot, "Robust constrained learning-based nmpc enabling reliable mobile robot path tracking," *The International Journal of Robotics Research*, vol. 35, no. 13, pp. 1547–1563, 2016.

[25] F. Berkenkamp, M. Turchetta, A. P. Schoellig, and A. Krause, "Safe model-based reinforcement learning with stability guarantees," *Advances in Neural Information Processing Systems 30*, vol. 2, pp. 909–919, 2018.

[26] J. F. Fisac, A. K. Akametalu, M. N. Zeilinger, S. Kaynama, J. Gillula, and C. J. Tomlin, "A general safety framework for learning-based control in uncertain robotic systems," *IEEE Transactions on Automatic Control*, vol. 64, no. 7, pp. 2737–2752, 2018.

[27] A. E. Bryson and Y. C. Ho, *Applied optimal control: optimization, estimation and control*. CRC Press, 1975.

[28] G. Cardano, T. R. Witmer, and O. Ore, *The rules of algebra: Ars Magna*. Courier Corporation, 2007, vol. 685.

[29] B. Chalaki, L. E. Beaver, and A. A. Malikopoulos, "Experimental validation of a real-time optimal controller for coordination of cavs in a multi-lane roundabout," in *31st IEEE Intelligent Vehicles Symposium (IV)*, 2020, pp. 504–509.

[30] A. I. Fleishman, "A method for simulating non-normal distributions," *Psychometrika*, vol. 43, no. 4, pp. 521–532, 1978.

[31] F. Pukelsheim, "The three sigma rule," *The American Statistician*, vol. 48, no. 2, pp. 88–91, 1994.